Kinetic analysis of capacity fade in lithium/coke half-cells

Neil R. Avery *, Krista J. Black

CSIRO Division of Materials Science and Technology, Private Bag 33, Clayton South MDC, Vic. 3169, Australia

Abstract

After prolonged cycling of a lithium/petroleum coke half-cell, a sudden and reversible voltage drop is often seen during the discharge cycle which leads directly to an apparent decrease in reversible lithium-ion intercalation capacity. Kinetic analysis of cells in this condition has been studied by complex impedance spectroscopy and current interruption. This has shown that the large increase in discharge resistance (~ 2.5 kΩ cm^2) is caused by an enlarged solid electrolyte interfacial (SEI) layer which increases both the migration resistance and the concomitant concentration polarisation in this layer. This effect has been attributed to passivation debris which has become dislodged from the electrode surfaces (probably the lithium counter) and migrates cataphoretically to, and blocks the carbon electrode during discharge. The appearance of this effect is regarded as a diagnostic indicator of the presence of this debris and should not be confused with a loss of reversible intercalation capacity. © 1997 Published by Elsevier Science S.A.

1. Introduction

For preliminary screening of new electroactive materials for both the negative and the positive electrodes of lithium-ion secondary batteries [1,2] it is convenient to cycle electrochemically the material in half-cells with a lithium metal counter electrode. Here, the counter electrode acts also as a reliable reference, eliminating the need for a separate reference electrode when the positive and negative electrode materials are assembled into a full lithium-ion battery configuration. In particular, electrochemical evaluation of these materials ranges from a determination of its intrinsic kinetics and thermodynamic capacity for reversible lithium-ion intercalation to its ability to maintain this performance after many charge and recharge cycles. As part of a materials evaluation of this kind, we have found that in lithium/petroleum coke half-cells a misleading impression of long-term intercalation capacity can arise from electrolyte deterioration, probably caused by the repeated cycling of the lithium counter electrode.

2. Experimental

Carbon electrodes were prepared from Lonza G&T 250-1500 petroleum needle coke which had been crushed and sieved to < 38 μm and air-winnowed to remove the fines. Electrodes were prepared by evenly spreading a slurry of 88% coke with 10% acetylene black and 2% ethylene propylene diene monomer in cyclohexane, with a doctor blade onto a cleaned 2 cm^2 copper current collector. The lithium counter electrode was cut from a lithium sheet and cleaned by etching in methanol. All materials and demountable stainless-steel cell parts were thoroughly dried before loading into an argon glovebox for cell assembly. During assembly, a Celgard 2500 microporous polypropylene separator was initially wetted with dimethyl carbonate (DMC) before flooding with 1 M LiPF$_6$ in 1:1 DMC/EC (ethylene carbonate) electrolyte.

Automated cell cycling and data acquisition at 21 °C was monitored and controlled by a Data Electronics DT505 data logger with a relay board. Cell voltages are recorded every 2–3 minutes, while a preset voltage limit of 1.5 V switched a constant ($\pm 2\%$) current supply from charge to discharge. Discharge was similarly limited to 0.02 V to prevent lithium plating on the carbon.

Complex impedance spectra were recorded at 21 °C with an EG&G PARC M6310 impedance spectrometer with a modulation potential of 5 mV rms. The total cell resistance, R_T, was determined from the difference between the operating cell potential and the open-circuit potential after current interrupt.

* Corresponding author.

3. Results and interpretation

After initial irreversible passivation during the first discharge [3], subsequent charge/discharge cycling of a typical petroleum coke electrode showed an initial reversible intercalation capacity of $Li_{x=0.55}C_6$ (205 mAh/g) at a discharge rate of 0.10 mA/cm². This was reduced to $x = 0.44$ at the higher rate of 0.83 mA/cm². Cycling was continued at a variety of rates for 1300 cycles. In this time, the slow rate showed a modest decrease in reversible capacity to $x = 0.44$, whereas at the higher rate of 0.83 mA/cm² the capacity decreased to $x = 0.12$ after 1300 cycles; the most rapid change was seen in the first 400 cycles (Fig. 1). The higher intercalation capacity could always be restored by reverting to the slower rate, indicating that the high rate capacity fade was of
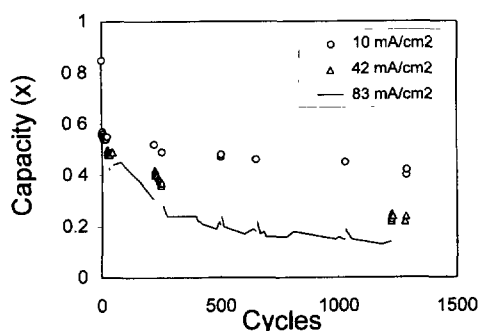

Fig. 1. Reversible lithium-ion intercalation capacity, x, of a petroleum coke electrode (5.6 mg/cm²) operating in a lithium half-cell configuration, plotted as a function of cycle number for three charge/discharge rates

a kinetic origin. This loss of capacity appeared to be a general phenomenon in long-term cycling of these half-cells, although the onset and magnitude of the effect could not be predicted from cell to cell.

A 0.1 mA/cm² charge/discharge voltage profile of a similar cell in the low capacity state is shown in Fig. 2. Here, when the cell voltage had fallen to 0.55 V there occurred a rapid fall of a further ~250 mV, corresponding to an increase in total cell resistance, R_T, of ~2.5 kΩ cm². The onset of this effect was rate dependent and occurred earlier in the discharge cycle at higher discharge rates. At lower rates the opposite effect was seen and at sufficiently low rates the cell never developed this condition and the full insertion capacity was restored. The rapid fall in cell voltage was always matched by a similarly rapid rise in voltage when the cell switched to the charge cycle. During both the charge cycle and that part of the discharge before the onset of the voltage discontinuity, current interruption indicated an overpotential of ~5 mV, corresponding to a total cell resistance R_T of ~50 Ω cm² (Table 1).

In this condition the cell could be changed back and forth between the high and low resistance states by switching between the discharge and charge currents, respectively. Furthermore, these states could be maintained indefinitely in the open-circuit condition, allowing complex impedance analysis of the two states. Complex impedance spectra of the cell in both the charge and the discharge states are shown as inserts in Fig. 2.
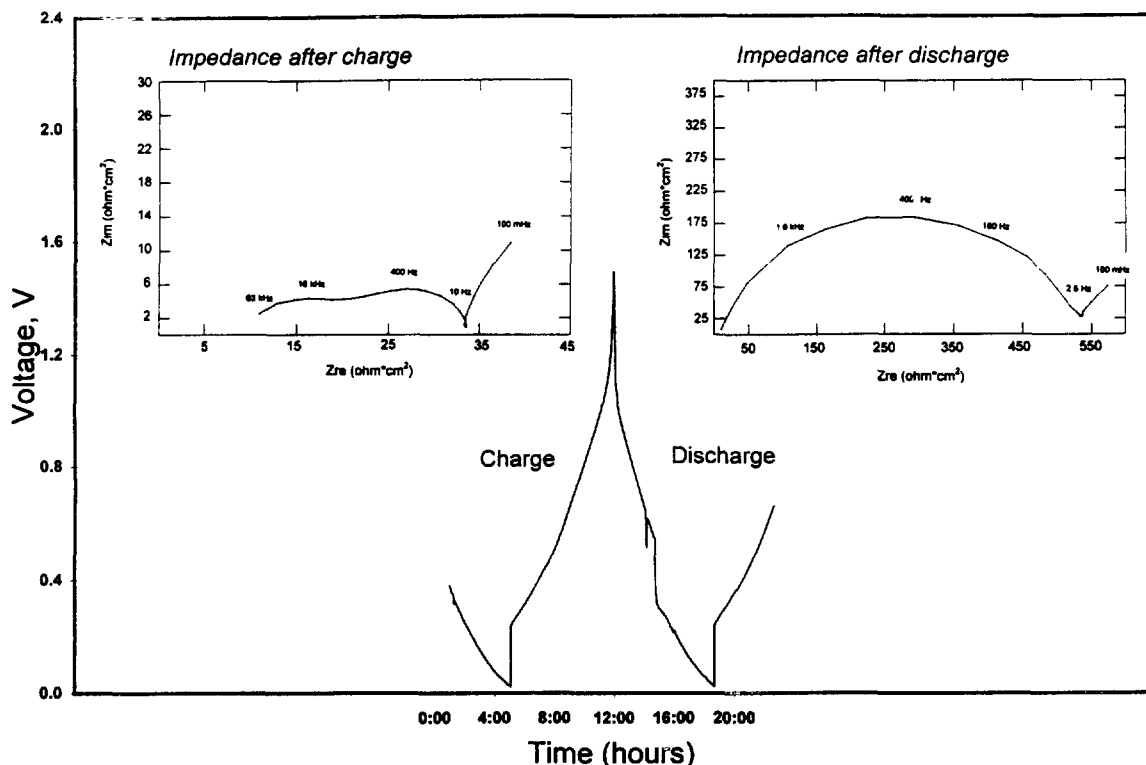

Fig. 2. Voltage profile of a petroleum coke electrode (6 mg/cm²), cycled in a lithium half-cell configuration (0.1 mA/cm²), after the capacity fade had been established The inserts show the complex impedance spectra with the cell in the charge and high resistance discharge states.

Table 1
Contributions to the cell resistance during charge and discharge of a coke vs. lithium half-cell

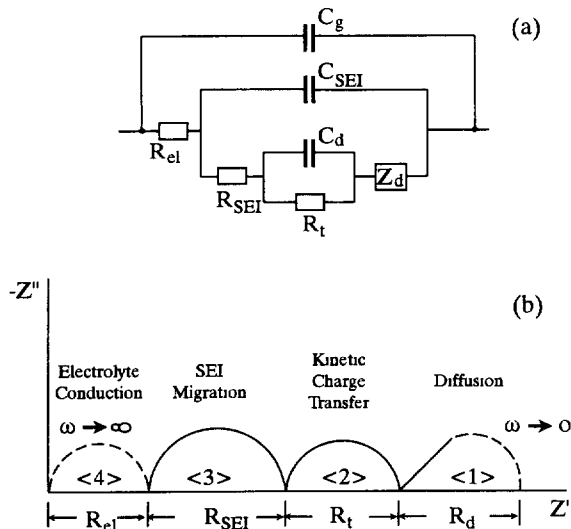| Process	Approximate resistance (Ω cm^2)		
	Symbol	Charge	Discharge
⟨1⟩ Diffusion	R_d	15	2000
⟨2⟩ Kinetic charge transfer	R_t	14	530 [a]
⟨3⟩ Migration in SEI layer	R_{SEI}	10	
⟨4⟩ Electrolyte conduction	R_{el}	10	10
Total	R_T	50	2500

[a] Predominantly migration.

Fig. 3. (a) Idealized equivalent circuit for a lithium battery with a passivating SEI layer; (b) impedance response in the complex plane.

The kinetics of processes limiting the performance of lithium batteries may be analysed by complex impedance spectroscopy. In a simplified treatment [4–6], four regions can be identified, and under favourable circumstances these will be resolved into clearly separated frequency domains as shown with an idealized equivalent circuit representation in Fig. 3. Arc ⟨2⟩ is seen in the medium frequency range and is determined by the kinetic charge-transfer impedance arising from the charge-transfer resistance, R_t, and the double-layer capacitance, C_d, in parallel with it. The remaining three regions are associated with mass-transport processes. At very high frequencies, the resistance intercept of ⟨4⟩ gives the ohmic resistance of the electrolyte, R_{el}. This very high frequency arc in the complex plane expected from coupling of R_{el} to the geometric capacitance, C_g, of the cell (typically pF/cm^2) is not usually seen when R_{el} is low, due to the limited higher frequency range of typical impedance spectrometers (< 100 kHz). Arc ⟨3⟩ is normally seen at high frequencies and arises from the migration impedance determined by the migration resistance, R_{SEI}, and capacitance of the surface electrolyte interfacial (SEI) layer, C_{SEI} (typically μF). Diffusion processes resulting from concentration polarisation are described by a Warburg impedance with a diffusion resis-

tance, R_d. This process occurs at low frequencies, but with a limiting frequency in the mHz regime, most impedance spectrometers reveal only the 45° tail of region ⟨1⟩. Instead, the diffusion resistance, R_d, can more conveniently be determined from the total cell resistance obtained by current interruption, R_T, according to

$$R_T = R_{el} + R_{SEI} + R_t + R_d \qquad (1)$$

Fouache-Ayoub et al. [5] have concluded that the concentration polarisation responsible for this diffusion resistance arises predominantly from within the SEI layer, where the electrolyte concentration can fall to a few percent of the bulk concentration.

Returning to the impedance spectra of the present cell, it is seen that in the charge state (Fig. 2) these four regions are clearly resolved. The high frequency resistance intercept due to R_{el} occurs at ~ 10 Ω cm^2, whereas arcs ⟨2⟩ and ⟨3⟩ are seen peaking near 400 Hz and 16 KHz, respectively, with resistance components due to charge transfer and SEI of 14 and 10 Ω cm^2, respectively. R_T was estimated by current interruption to be ~50 Ω cm^2, leaving ~ 15 Ω cm^2 of diffusion resistance at the operating current density, viz. 0.1 mA/cm^2, Table 1.

In the discharge state, the complex impedance spectrum (Fig. 2) showed a high frequency resistance R_{el} of ~ 10 Ω cm^2 similar to that seen in the charge state. The greatly increased cell resistance seen in the discharge voltage curve (Fig. 2) failed to show a resolved pair of arcs ⟨2⟩ and ⟨3⟩ in the impedance spectrum and instead was characterized by a single arc at 400 Hz which precluded a meaningful separation of the magnitude of the migration and charge-transfer resistances. The sum of the electrolyte, migration and charge-transfer resistances amounted to 540 Ω cm^2, leaving, according to Eq. (1), ~ 2 kΩ cm^2 of diffusion resistance (Table 1). It is unlikely that the charge-transfer processes would be affected significantly by the charge/discharge state of the cell, in which case most of the 540 Ω cm^2 of cell resistance is likely dominated by migration effects in an enhanced SEI layer.

4. Discussion

Comparison of the reversible capacity with low cycling currents immediately after the initial passivation and again after 1300 cycles showed a 20% loss. At higher currents, the 80% loss of reversible capacity must be attributed to kinetic effects as seen by the large increase in cell resistance during the discharge cycle which appears to be localized in the SEI layer.

It is well known that both the negative and positive electrodes in these lithium half-cells must be passivated by decomposition of electrolyte solvent to form a protective SEI layer. For the lithium negative electrode, this occurs spontaneously after cell assembly [7], whereas the carbon electrode is passivated by electrochemical degradation of the electro-

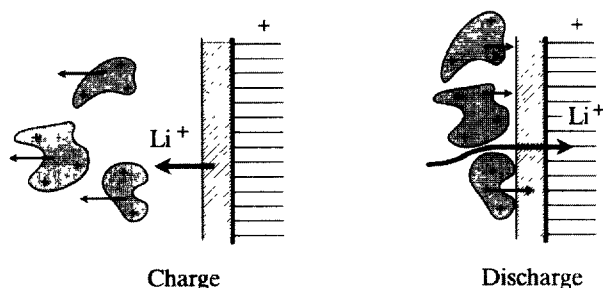**Charge**   **Discharge**

Fig. 4. Model showing the electrophoretic migration of positively charged (from coordinated lithium ions) electrolyte decomposition debris resulting from repeated charge and discharge cycles of a coke vs. lithium half-cell. During discharge this debris may accumulate at and partially block the migration of lithium ions to the coke electrode.

lyte as the carbon potential drops to ~0.8 V during the first discharge [3]. With repeated cycling, any deterioration of the SEI layer will automatically be repaired by further solvent degradation. In particular, the lithium counter electrode is being continuously oxidized and replated as high surface area dendrites, giving an opportunity for further generation and subsequent detachment of SEI material into the electrolyte. Analysis of the material making up the SEI layer indicates a range of compounds, all of which are oxygen rich [8]. This material may be expected to coordinate to lithium ions and, once dislodged, migrate cataphoretically with, but more sluggishly than the lithium ions.

Accordingly, the model to account for the effect described here is that slow cataphoretic migration of this material occurs along with the lithium ions to the carbon electrode during discharge (Fig. 4). Drift of this material in the field will be subject to competing thermal motion, so that at low currents it does not accumulate at either electrode. At higher discharge currents, cataphoretic drift prevails and this detached debris may accumulate at the carbon electrode during discharge leading directly to a significant increase in lithium-ion migration and associated concentration polarisation resistances of the cell. On recharge, this material will migrate away from the carbon electrode and, by not obstructing the transport of lithium ions, restores the lower cell resistance. During the charge cycle this material has the same opportunity to accumulate on the lithium electrode, but does not lead to a high

cell resistance, presumably due to the higher real surface area of this electrode.

This same effect has more recently been seen with $LiMn_2O_4$ electrodes cycled in lithium half-cell configurations. After many cycles, a sudden voltage drop similar to that reported above amounting to an increased R_T of several $k\Omega\ cm^2$ develops during discharge. For a cell in this condition, the normal early cycle voltage profile has been restored by dismantling and reassembling the cell with fresh electrolyte and lithium counter electrode [9], in general agreement with the thesis that an increased discharge cell resistance is associated with electrolyte degradation.

In conclusion, the appearance of an otherwise inexplicable rapid voltage decrease during discharge in a lithium half-cell appears to be a diagnostic indicator that the electrolyte has become contaminated with SEI-derived debris dislodged from the lithium counter electrode, and that any resulting reversible capacity loss is not necessarily due to a failure of the working electroactive material.

Acknowledgements

References

[1] G. Pistoia (ed.), Lithium Batteries, New Materials, Developments and Perspectives, Elsevier, Amsterdam, 1994.

[2] J. Broadhead and M. Farley, J. Power Sources, 54 (1995) and Refs. therein.

[3] R. Fong, U. Von Sacken and J.R. Dahn, J. Electrochem. Soc., 137 (1990) 2009.

[4] P.R. Sorensen and T. Jacobsen, Electrochim. Acta, 27 (1982) 1671

[5] S. Fouache-Ayoub, M. Garreau, P.V.S.S. Prabhu and J. Thevenin, J. Electrochem. Soc., 137 (1990) 1659.

[6] D. Rahner, S. Machill and G. Ludwig, J. Power Sources, 54 (1995) 378.

[7] E. Peled, J. Electrochem. Soc., 126 (1979) 2047

[8] D. Aurbach, A. Zaban, Y. Gofer, Y.E. Ely, I. Weissman, O. Chusid and O. Abramson, J. Power Sources, 54 (1995) 76.

[9] N.R. Avery and K.J. Black, unpublished data.